International Journal of Innovation in
Mechanical Engineering and Advanced Materials
Vol. 6 (No. 1). 2024. pp. 22-37
Journal homepage: publikasi.mercubuana.ac.id/index.php/ijimeam
DOI: 10.22441/ijimeam.v6i1.18915

Optimized Frame Design for Head Loss Testing Equipment Through Material Strength Analysis

Hendrikus Wermasaubun [1,*], Muhamad Fitri [1], Abdul Hamid [2] and Dedik Romahadi [1,3]

[1]Department of Mechanical Engineering, Faculty of Engineering, Universitas Mercu Buana, Jakarta 11650, Indonesia
[2]IM Tech Focus Group, Faculty of Technical Vocational Education, University Tun Hussein Onn Malaysia, Johor 86400, Malaysia
[3]School of Material Science and Technology, Beijing Institute of Technology, Beijing 100811, China
*Corresponding Authors: wermasaubunh@gmail.com (HW)

Abstract

This article presents the design and analysis of a frame for head loss testing equipment, crucial for evaluating flow losses in pipe installations. The objective was to develop a robust yet lightweight frame that could withstand the operational loads imposed by the testing equipment. The frame, which supports essential components such as pipes, venturi meters, elbows, and reducers, was constructed using ASTM A500 hollow sections with dimensions of 20 x 20 x 1.6 mm and 35 x 35 x 1.6 mm. These dimensions were selected for their balance between strength and weight, validated through strength analysis and SolidWorks simulations. Conducted at Universitas Mercu Buana, the project involved the design, manufacturing, and testing of the frame to determine its load-bearing capacity. The results from the SolidWorks simulations confirmed the frame's structural integrity, which was further validated by its successful application in a practical setup. This study demonstrates the effectiveness of a systematic design approach, integrating material selection, load analysis, and simulation to achieve an optimal solution. The findings contribute valuable insights into the use of ASTM A500 hollow sections in structural applications, particularly where both strength and weight are critical. This work sets a precedent for future designs in mechanical engineering, offering a reliable framework for developing durable and efficient testing equipment.

Article Info:
Received: 28 March 2023
Revised: 30 August 2023
Accepted: 3 June 2024
Available online: 30 August 2024

Keywords:
Head loss testing equipment; structural frame design; material strength analysis; SolidWorks simulation; ASTM A500 hollow sections

1. Introduction

Piping systems play a crucial role in fluid distribution across various applications, offering an efficient means of transporting fluids from one location to another. These systems can range from simple, single-pipe configurations to complex, branched networks, all of which require a variety of fittings such as strainers, valves, taps, joints, elbows, and reducers. However, these components can introduce energy losses in the form of minor losses due to local disturbances like changes in cross-sectional area or directional turns, and major losses caused by friction between the fluid and the pipe walls [1]. Analyzing these losses is challenging because fluid flow within pipes is not directly visible, which complicates the assessment and optimization of the system's performance [2][3].

To address this, head loss testing equipment is used to measure and evaluate the flow losses within pipe installations. The frame that supports this testing equipment must be carefully designed to withstand the loads imposed by the system while remaining lightweight and flexible [4] [5]. The design process involves selecting appropriate materials, considering the strength and balance of the frame, and applying methods such as the VDI 2221 design methodology [6] [7], material strength analysis [8], and software simulations like SolidWorks [9] [10]. These approaches ensure that the frame is robust enough to support the equipment during testing while maintaining the necessary structural integrity and performance.

The frame's design must accommodate the dynamic nature of the loads during testing, which requires not only strength but also flexibility to absorb any shocks or vibrations that may occur. This balance between strength and flexibility is critical to ensure the accuracy and reliability of the head loss measurements. Material selection plays a vital role in achieving this balance, with the choice of materials being guided by their ability to withstand the expected stresses while minimizing weight.

How to cite:

H. Wermasaubun, M. Fitri, A. Hamid, and Dedik Romahadi, "Optimized frame design for head loss testing equipment through material strength analysis," *Int. J. Innov. Mech. Eng. Adv. Mater*, vol. 6, no. 1, pp. 22-37, 2024

The application of material strength analysis allows designers to calculate and predict the behavior of the frame under different load conditions, ensuring that it meets the necessary safety factors.

Moreover, the use of software simulations, such as those performed with SolidWorks, enhances the design process by providing a virtual environment to test and refine the frame before physical prototypes are built. These simulations can model complex scenarios, including the interaction of various components within the frame, and can predict potential points of failure or areas where the design could be optimized. By integrating these advanced tools and methodologies, the design of the head loss testing equipment's frame can be tailored to meet specific operational requirements, ensuring both durability and performance.

2. Methods

The research methodology for designing the frame of the head loss testing equipment is structured to ensure a robust and efficient design that meets all operational requirements. The process begins with the application of material strength analysis to understand the fundamental properties and behaviors of the materials under load. This analysis is crucial for identifying, calculating, and evaluating the forces and stresses that the frame will encounter during operation.

The frame design process began with a material strength analysis, followed by detailed design calculations to ensure the structure could withstand the anticipated loads [11][12]. Based on these analyses, specifications were carefully selected to meet the necessary requirements [13], and the final frame design was developed accordingly, as shows in Figure 1.

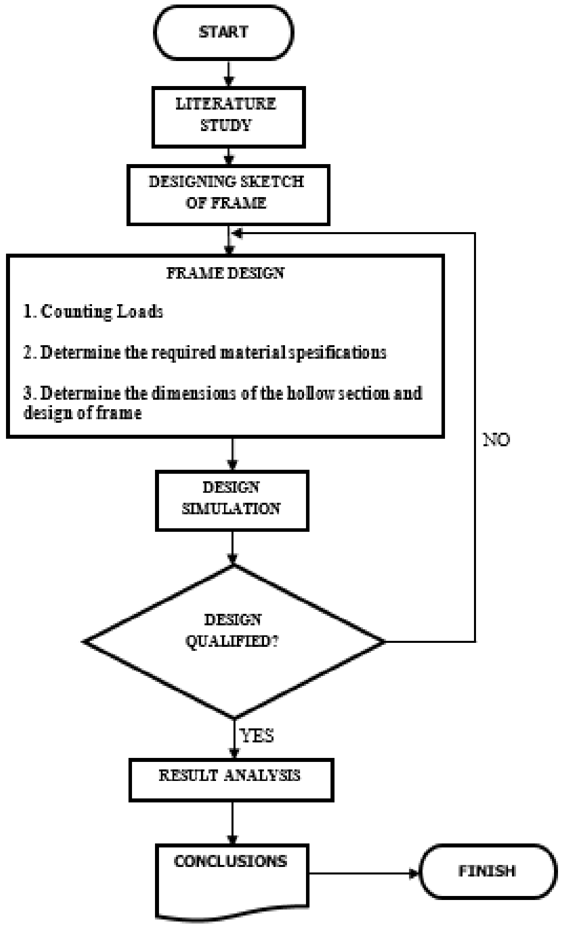

Figure 1. Design flowchart

The design process follows a systematic approach, starting with the conceptual design of the frame, as shown in Figure 1. Initial design sketches are created based on the requirements of the head loss testing equipment, including the need for strength, lightness, and structural stability. Various design iterations are considered, and the most suitable design is selected based on a balance of these factors.

Following the conceptual design phase, detailed calculations are performed to determine the specific loads that the frame must support. These calculations involve assessing the mass of the frame, the components of the head loss testing equipment, and the fluid load within the system. The strength and flexibility of the frame are then evaluated using established engineering formulas and principles, ensuring that the frame can withstand the expected loads with an adequate safety margin.

To refine and validate the design, software simulations are conducted using tools such as SolidWorks. These simulations model the load conditions and structural behavior of the frame under different scenarios, allowing for the optimization of the design. The simulations also help identify potential weak points in the frame, which can be addressed before physical construction.

Once the design has been thoroughly analyzed and optimized, the final specifications for the frame are determined. This includes selecting appropriate materials, such as ASTM A500 hollow sections, and specifying the dimensions and cross-sectional properties required to achieve the desired strength and weight characteristics. The frame design and loading mass data were shown in Figure 2 and Table 1, respectively.

The final step in the methodology involves the construction and testing of the frame. The constructed frame is subjected to physical load tests to verify its performance against the design simulations. Any discrepancies between the simulated and actual performance are analyzed, and adjustments are made as necessary to ensure the frame meets all design criteria.

The strength analysis method is expected to understand the basics of inner material strength related to the design process, Identify, calculate and analyze force phenomena that occur in a component construction, the method helps the process of designing a frame construction and can optimize designer to find the accurate design [14][15][16][17].

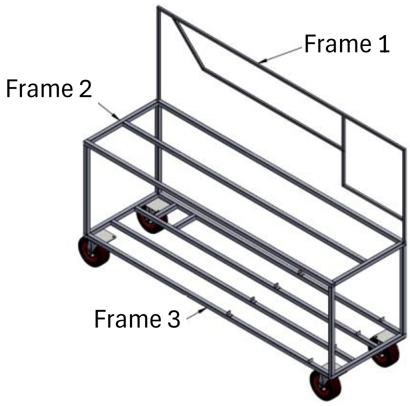

Figure 2. Frame design

Table 1. Loading mass data

Component	Mass [kg/m] or [kg]
Hollow 20 x 20 x 1.6 [mm]	0.87 [kg/m]
Hollow 35 x 35 x 1.6 [mm]	1.63 [kg/m]
PVC Pipe	0.315 [kg/m]
Water Bath	249.25 [kg]
Pump	13 [kg]
Pressure Gauge	0.75 [kg]
Tee	0.105 [kg]
Valve	0.22 [kg]
Fountain	0.65 [kg]
Elbow	0.07 [kg]
Reducer	0.11 [kg]
Galvanized Pipe	2.50 [kg/m]
Stainless Steel Pipe	1.30 [kg/m]

3. Results and Discussion

The sketch provided illustrates the loading on a vertical rod, as shown in Figure 4, commonly found in structural frameworks. In this particular figure, the vertical rod is subjected to two forces.

FkA: This force represents the load applied at the top of the vertical rod.

Ra: This force acts as a reaction force at the base of the vertical rod.

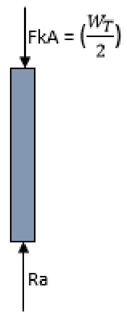

Figure 3. Sketch of vertical rods loading

To determine the safety factor, some considerations were evaluated as follows

W_T = 7 elbow + 8 tee + 1 valve + 2 faucet + 2 pipe 1.5 inch (0.13 [m]) + 2 pipe 1 inch (0.42 [m])

W_T = 7 (0.07) + 8 (0.105) + 0.220 + 2 (0.650) + 2 (0.1) + 2 (0.132) = 3.314 kg

$$\sigma_y = 315 \text{ MPa}$$

$$Fs = 2$$

Afterwards, the area can be calculated as

$$\text{FkA} = (\frac{3.314}{2}) = 1.657 \text{ kg} = 16.57 \text{ [N]}$$

$$\sigma_{allowed} = \frac{315}{2} = 157.5 \text{ Mpa}$$

$$A_{calculated} = \frac{1,657}{157,5} = 0,1052 \text{ [mm}^2\text{]}$$

So, the selected A_{table} is 102 [mm^2] with a hollow size 20 x 20 x 1.6 SHS.

In general, the key aspects of a horizontal rod loading sketch include the following:

Applied Load (F): This represents the external force or forces acting on the horizontal rod. These loads could be distributed along the length of the rod or concentrated at specific points.

Support Reactions (Ra and Rb): At the ends of the horizontal rod, support reactions arise in response to the applied loads.

Bending Moment Diagram: A bending moment diagram might be included in a more detailed sketch to show how the moment varies along the length of the rod. This diagram shows the internal stresses and ensures the rod's material can withstand these stresses without failure.

Shear Force Diagram: Similarly, a shear force diagram may accompany the sketch, illustrating how shear forces vary along the rod. Shear forces can cause sliding failure between sections of the rod, so it's essential to visualize these forces to ensure structural safety.

Deflection Curve: The deflection curve, representing how the rod bends under the applied load.

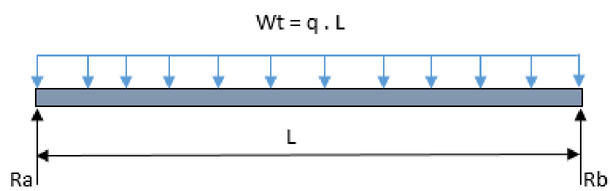

Figure 4. Sketch of horizontal rods loading for Frame 1

Finding the bending stress value, can be calculated as:

$$Wt = 3.314\ [kg] = 33.14\ [N]$$

$$L = 250\ [mm]$$

$$M = \frac{1}{8}\ .\ 33.14\ .\ 250$$

$$M = 1035.63\ [N.mm]$$

$$Z_{calculated} = \frac{1035.63}{157.5} = 6.5339\ [mm^3]$$

So, the selected Z_{table} is 0.570 x 10^3 [mm^3] with a hollow size 20 x 20 x 1.6 SHS

The load simulation for rods (1A, 1B, and 1C) using SolidWorks were conducted to visualize the load concentration.

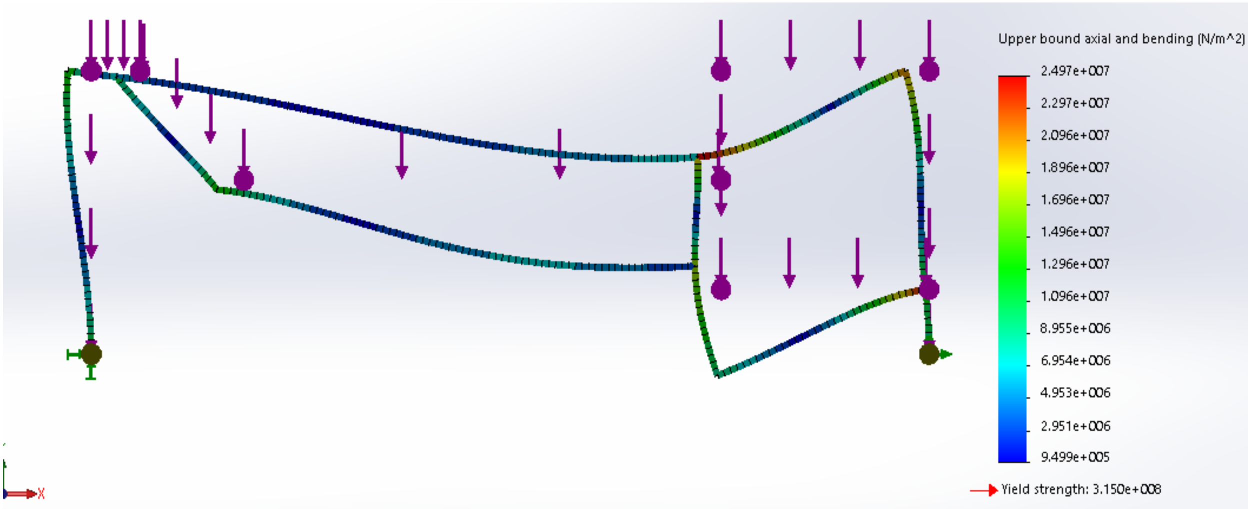

Figure 5. Sketch of frame 1 using SolidWorks

Loading sketch for rods (2A, 2B, and 2C)

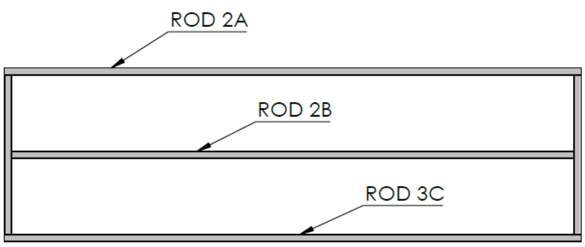

Figure 6. Sketch of horizontal rods 2A, 2B, and 2C) for Frame 2

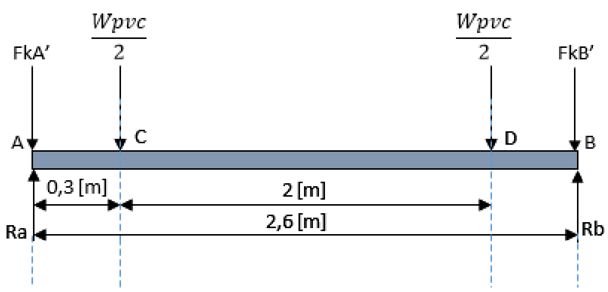

Figure 7. Sketch of horizontal rods loading

$$q_{pipe}\,\text{PVC} = 0.315\ [\text{kg/m}] = 0.00315\ [\text{N/mm}]$$

$$L = 200\ [\text{mm}]$$

$$\text{FkA'} = \frac{4.73\ [\text{m}].0.87\ [\text{kg/m}] + 3.314\ [\text{kg}]}{2} = 3.7145\ [\text{kg}] = 37.145\ [\text{N}]$$

Calculation step:

$$\Sigma Mb = 0$$

$$Ra \,.\, 2.6 - \text{FkA'} \,.\, 2.6 – 3.15 \,.\, 0.3 – 3.15 \,.\, 2.3 = 0$$

$$Ra = 40{,}295\ [\text{N}]$$

$$\Sigma Fv = 0$$

$$40.295 + Rb = 3.15 + 3.15 + 37.145 + 37.145$$

$$Rb = 40{,}295\ [\text{N}]$$

$$Mc = Ra \,.\, 0{,}3 = 12{,}0085\ [\text{N.m}]$$

$$Md = Rb \,.\, 0{,}3 = 12{,}0085\ [\text{N.m}]$$

Latitude and moment diagram were shown as following.

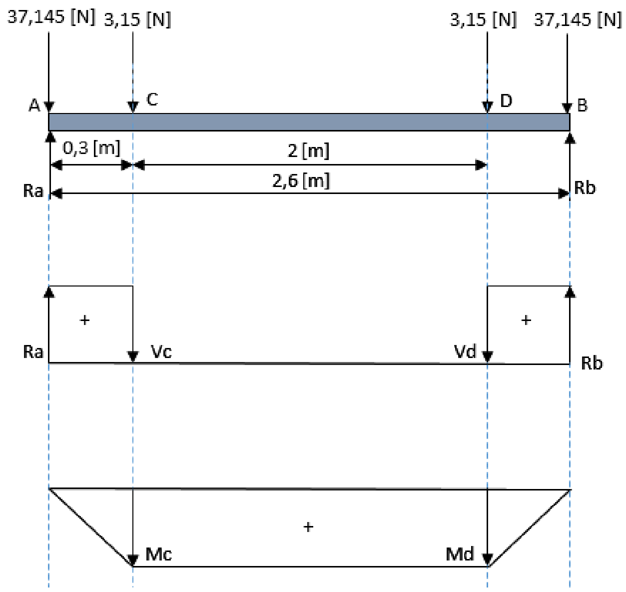

Figure 8. Latitude and moment diagram

$$Z_{calculated} = \frac{12{,}0085 \times 10^3}{157{,}5} = 0{,}07624 \times 10^3\ [\text{mm}^3]$$

So, the selected Z_{table} is 2,00 x 10^3 [mm^3] with a hollow size 35 x 35 x 1.6 SHS

Sketch of horizontal rod loading 2A (galvanized pipe), were described as follows.

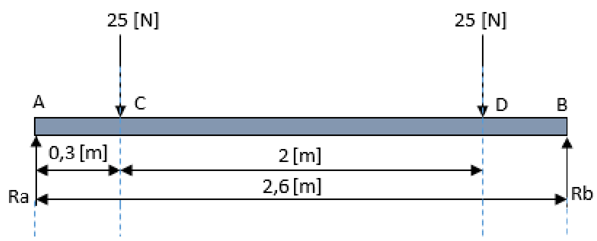

Figure 9. Sketch of horizontal rods loading

were;

$$q_{Galvanized\_pipe} = 2.50\ [kg/m] = 0.0250\ [N/mm]$$

$$L = 200\ [mm]$$

calculation step:

$$\Sigma Mb = 0$$

$$Ra\ .\ 2{,}6 - 25\ .\ 0{,}3 - 25.\ 2{,}3 = 0$$

$$Ra = 25$$

$$\Sigma Fv = 0$$

$$Ra + Rb = 25 + 25$$

$$Rb = 25\ [N]$$

$$Mc = Ra\ .\ 0{,}3 = 0{,}75\ [N.m]$$

$$Md = Rb\ .\ 0{,}3 = 0{,}75\ [N.m]$$

The latitude and moment diagram are shown below.

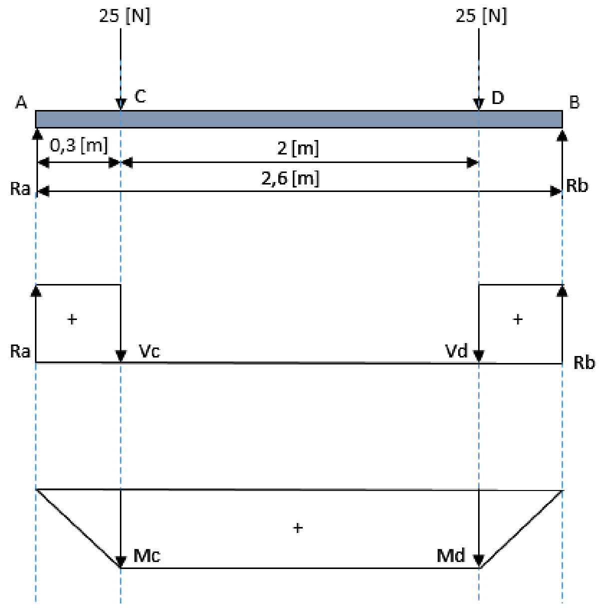

Figure 10. Latitude and moment diagram

$$Z_{Calculated} = \frac{0{,}75\ x\ 10^3}{157{,}5} = 0{,}0047\ x\ 10^3\ [mm^3]$$

So, the selected Z_{table} is 2,00 x 103 [mm3] with a hollow size 35 x 35 x 1.6 SHS
The sketch of horizontal rod loading 2A (galvanized pipe) is shown below.

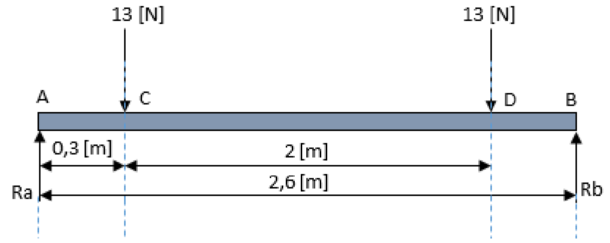

Figure 11. Sketch of horizontal rods loading

were;

$$q_{pipa} \text{ alumunium} = 1.30\ [kg/m] = 0.0130\ [N/mm]$$

$$L = 200\ [mm]$$

calculation step:

$$\Sigma Mb = 0$$

$$Ra\ .\ 2.6 - 13\ .\ 0.3 - 13\ .\ 2.3 = 0$$

$$Ra = 13$$

$$\Sigma Fv = 0$$

$$Ra + Rb = 13 + 13$$

$$Rb = 13\ [N]$$

$$Mc = Ra\ .\ 0.3 = 0.69\ [N.m]$$

$$Md = Rb\ .\ 0.3 = 0.69\ [N.m]$$

The latitude and moment diagram are shown below.

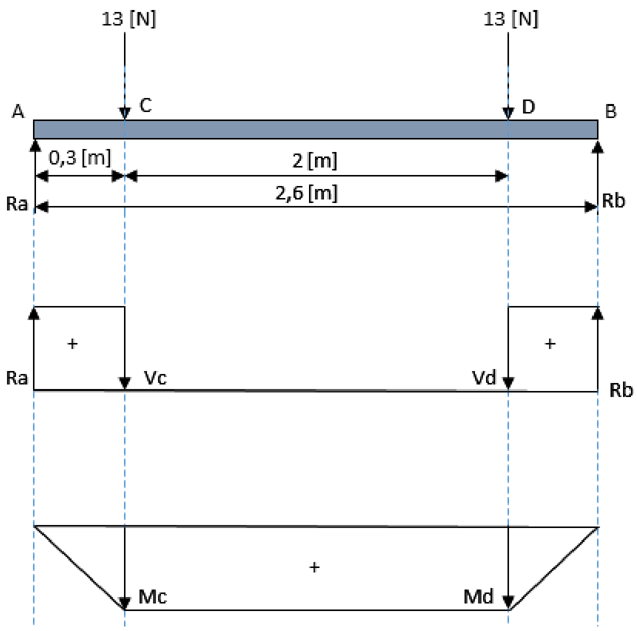

Figure 12. Latitude and moment diagram

$$Z_{hitung} = \frac{0,69\ x\ 10^3}{157,5} = 0,0043 \times 10^3\ [mm^3]$$

So, the selected Z_{table} is 2,00 x 10^3 [mm^3] with a hollow size 35 x 35 x 1.6 SHS

The sketch of vertical rod loading for Frame 2 is described in Figure 13.

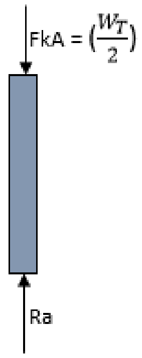

Figure 13. Sketch of vertical rods loading

were;

$$W_T = W_{Frame\_1} + W_{pvc} + W_{galvanized\_pipe} + W_{alumunium} + W_{Frame\_2}$$

$$W_T = 3.7145\ [kg] + 0.315\ [kg] + 5\ [kg] + 2.6\ [kg] + 1.63\ [kg/m]\ .\ 9.4\ [m]$$

$$W_T = 26.9515\ [kg]$$

$$\sigma_y = 317\ MPa$$

$$Fs = 2$$

Thus;

$$FkA = (\frac{26.9515}{4}) = 6.7378\ [kg] = 67.378\ [N]$$

$$\sigma_{allowed} = \frac{317}{2} = 157.5\ Mpa$$

$$157.5 = \frac{67.372}{A_{Calculated}}$$

$$A_{Calculated} = \frac{67.372}{157.5} = 0.4277\ mm^2$$

So, the selected A_{table} is 189 [mm^2] with a hollow size 35 x 35 x 1.6 SHS.

The load simulation for horizontal rods (2A, 2B, and 2C) using SolidWorks is shown below.

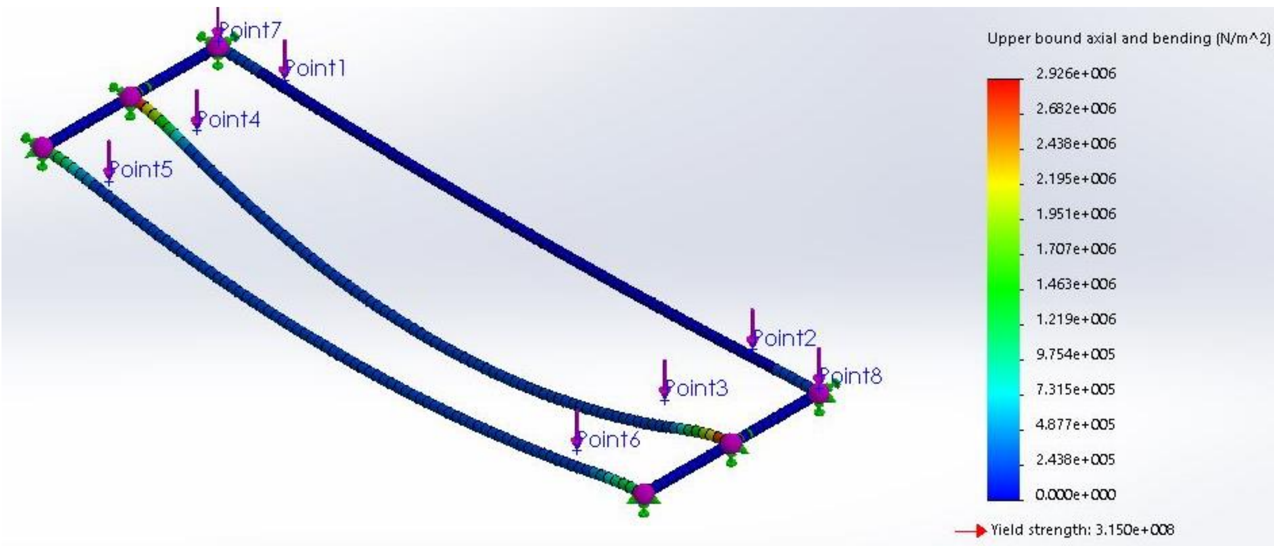

Figure 14. Sketch of frame 2 using SolidWorks for Frame 2

The loading sketch for rods (2A, 2B, and 2C) for Frame 3 is described below.

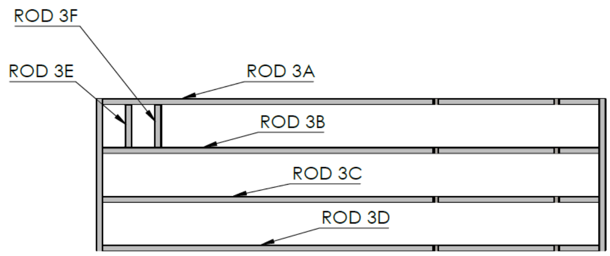

Figure 15. Sketch of horizontal rods 3A, 3B, 3C and 3D) for Frame 3

As the sketch of horizontal rod loading result shown below.

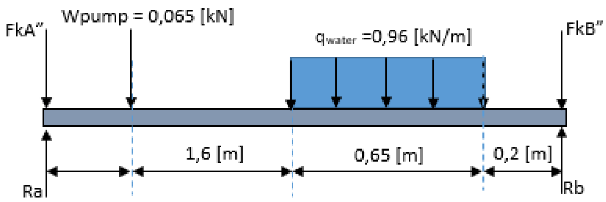

Figure 16. Sketch of horizontal distributed load rods

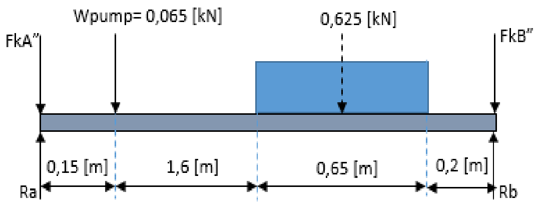

Figure 17. Sketch of horizontal concentrated load rods

were;

FkA" = FkB"

$$FkA" = \frac{26{,}9515\,[kg] + 1{,}63\,[kg/m]\,.3{,}2\,[m]}{4}$$

$$FkA" = 8{,}0418\,[kg] = 80{,}418\,[N] = 0{,}080418\,[kN]$$

$$\Sigma M_A = 0$$

$$Rb\,(2{,}6) - 0{,}625\,(2{,}175) - 0{,}065\,(0{,}15) - FkB"\,(2{,}6) = 0$$

$$Rb = 0{,}6069\,[kN]$$

$$\Sigma Fy = 0$$

$$Ra + 0{,}6069 - 0{,}065 - 0{,}625 - 0{,}080418 - 0{,}080418 = 0$$

$$Ra = 0{,}2439\,[kN]$$

Thus;

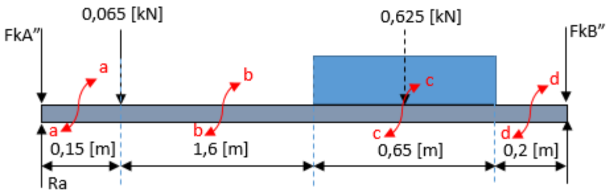

Figure 18. Sketch of horizontal rods with section

3.1. Strength analysis of section a-a

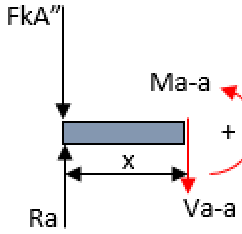

Figure 19. Section a-a

The calculated results are shown as follows.

$$\Sigma Fy = 0$$

$$Ra - FkA'' - Va\text{-}a = 0$$

$$Va\text{-}a = Ra - FkA'' = 0.2439 - 0.080418 = 0.1634 \text{ [kN]}$$

$$\Sigma Ma = 0$$

$$Ma\text{-}a - Va\text{-}a\,(x) \quad = 0$$

$$Ma\text{-}a = 0.1634\,(x)$$

$$(0 \leq x \leq 0{,}15.) \text{ m}$$

$$x = 0;\ Ma\text{-}a = 0.1634\,(0) = 0$$

$$x = 0{,}15;\ Ma\text{-}a = 0.1634\,(0{,}15) = 0.02451 \text{ [kN.m]}$$

3.2. Strength analysis of section b-b

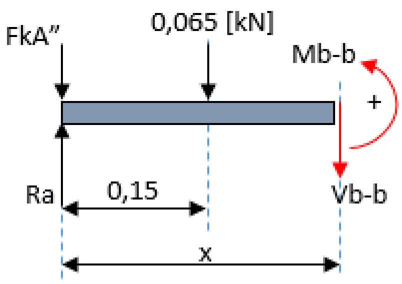

Figure 20. Section b-b

The calculated results are shown as follows.

$$\Sigma Fy = 0$$

$$Ra - FkA'' - Vb\text{-}b - 0.065 = 0$$

$$Vb\text{-}b = 0.2439 - 0.080418 - 0.065$$

Vb-b = 0.0984 [kN]

ΣMa = 0

Mb-b – Vb-b (x) – 0.065(0.15) = 0

Mb-b = 0.0984 (x) + 0.00975

(0.15 ≤ x ≤ 1.75) m

x = 0.15; Mb-b = 0.0984 (0.15) + 0.00975 = 0.02451 [kN.m]

x = 1.75; Mb-b = 0.0984 (1.75) + 0.00975 = 0.18195 [kN.m]

3.3. Strength analysis of section c-c

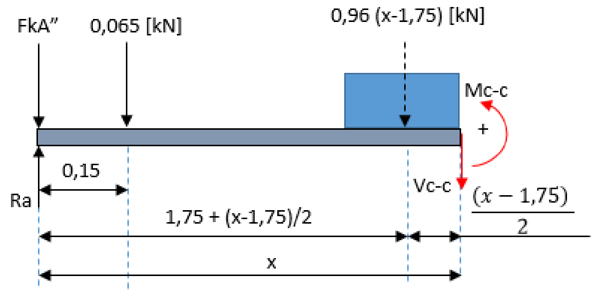

Figure 21. Section c-c

The calculated results are shown as follows.

ΣFy = 0

Ra – FkA" – Vc-c – 0.065 – 0.96 (x-1.75) = 0

Vc-c = 0.0984 – 0.96 (x-1.75) = 0

(1.75 ≤ x ≤ 2.4) m

x = 1.75; Vc-c= 0.0984 – 0.96 (1.75-1.75)

x = 1.75; Vc-c= 0.0984 [N]

x = 2.4; Vc-c = 0.0984 – 0.96 (2.4 – 1.75)

x = 2.4; Vc-c = -0.5256 [N]

ΣMa = 0

Mc-c – Vc-c (x) – 0.96(x-1.75) $\left(1.75 + \frac{x-1.75}{2}\right)$ – 0.065 (0.15) = 0

x = 1.75; Mc-c = (0.0984 – 0.96 (1.75-1.75)) (1.75) + 0.96 (1.75-1.75) $\left(1.75 + \frac{1,75-1,75}{2}\right)$ + 0.00975

Mc-c = 0.18195 [kN.m]

x = 2,4; Mc-c = (0.0984 – 0.96 (2.4-1.75)) (2.4) + 0.96 (2,4-1,75) $\left(1,75 + \frac{2,4-1,75}{2}\right)$ + 0,00975

Mc-c = 0,04311 [kN.m]

Finding the value (x) for the maximum moment:

Mc-c = (0.0984 – 0.96 (x-1.75)) (x) + 0.96 (x-1.75) $\left(1.75 + \frac{x-1.75}{2}\right)$ + 0.00975

Mc-c = (- 0.48x^2 + 1.7784x – 1.46025)

Mc-c' = (- 0.96x + 1.7784)

$$x = \frac{1{,}7784}{0{,}96} = 1{,}8525\ [m]$$

Finding the maximum moment:

$$\Sigma Ma = 0$$

$$x = 1.8525;\ Mc\text{-}c = (0.0984 - 0.96\,(1.8525\text{-}1.75))\,(1.8525) + 0.96\,(1.8525\text{-}1.75)\left(1.75 + \frac{1.8525-1.75}{2}\right) + 0.00975$$

$$x = 1.8525;\ Mc\text{-}c = 0.186993\ [kN.m] = 0.186993 \times 10^6\ [N.mm]$$

3.4. Strength analysis of section d-d

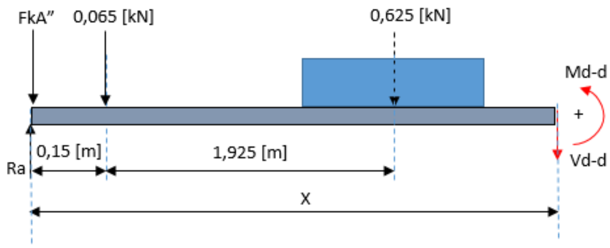

Figure 22. Section d-d

The calculated results are shown as follows.

$$\Sigma Fy = 0$$

$$Ra - FkA'' - 0.065 - 0.625 - Vd\text{-}d = 0$$

$$Vd\text{-}d = -\ 0.5265\ [kN]$$

$$\Sigma Ma = 0$$

$$Md\text{-}d - Vd\text{-}d\ (x) - 0.625\ (0.15 + 1.925) - 0{,}065(0.15) = 0$$

$$Md\text{-}d = -\ 0.5265\ (x) + 1.306625$$

$$(2.4 \le x \le 2.6)\ m$$

$$x = 2.4;\ Md\text{-}d = -\ 0.5265\ (2.4) + 1.306625 = 0.0429\ [kN.m]$$

$$x = 2.6;\ Md\text{-}d = -\ 0.5265\ (2.6) + 1.306625 = -\ 0.0622\ [kN.m]$$

Finding allowed stress strength as follows.

$$\sigma_{allowed} = \frac{\sigma_y}{F_s}$$

$$\sigma_{allowed} = \frac{315}{2} = 157{,}5\ Mpa$$

finding $Z_{calculated}$:

$$Z_{cal} = \frac{M_{max}}{\sigma_{cal}} = \frac{186993}{157{,}5} = 1{,}187\ x\ 10^3\ [mm^3]$$

So, the selected Z_{table} is 2,00 x 10^3 [mm^3] with a hollow size 35 x 35 x 1.6 SHS

The load simulation results for horizontal rods (3A, 3B, 3C, 3D, 3E, and 3F) using SolidWorks is shown below. And the load simulation results for frame head loss testing equipment shown in Figure 26.

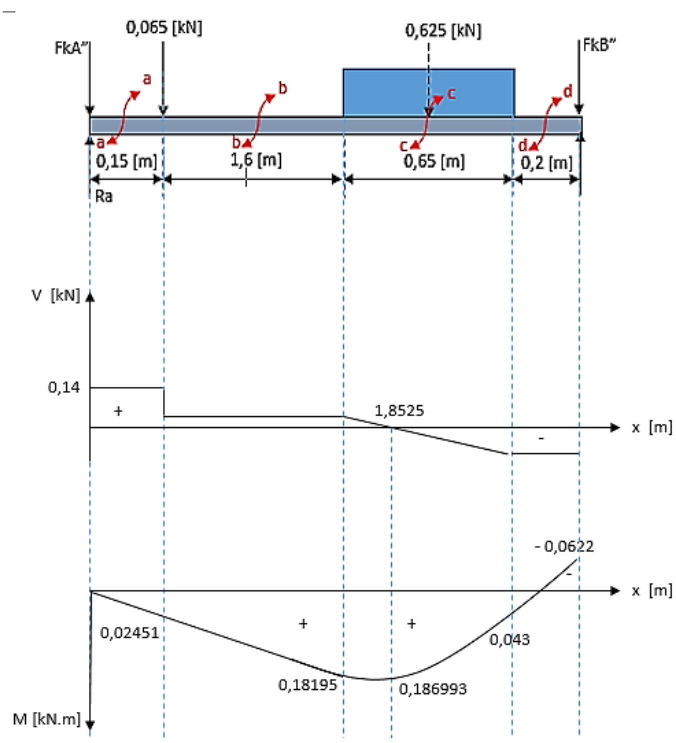

Figure 23. Latitude and moment diagram

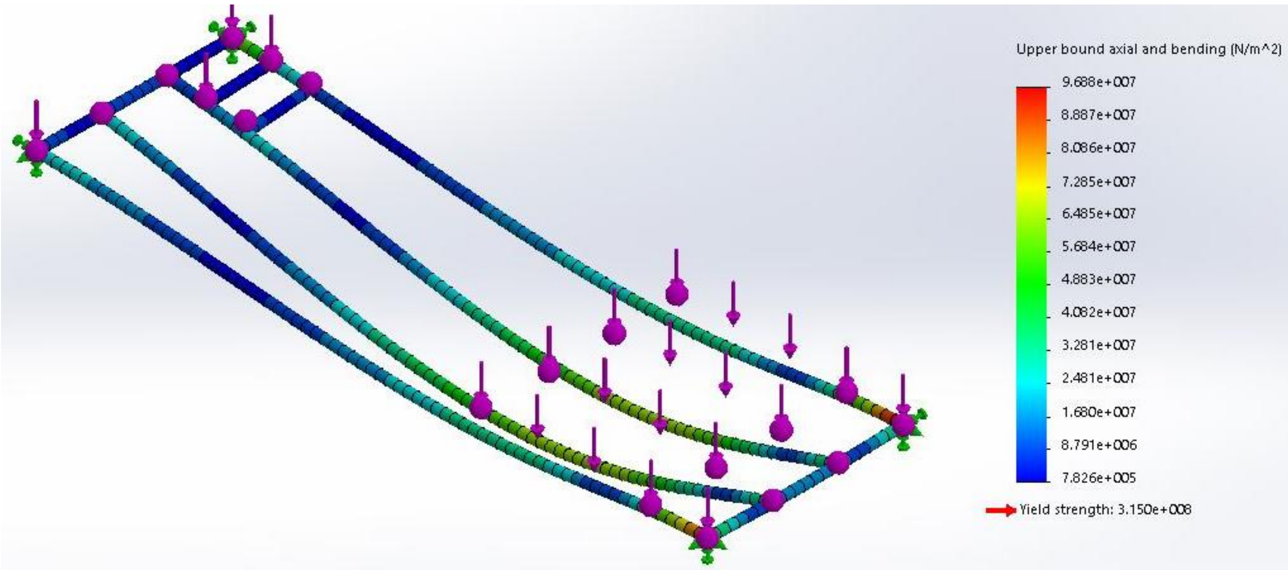

Figure 24. Load simulation for horizontal rods (3A, 3B, 3C, 3D, 3E, and 3F) of Frame 3

3.5. Loadings for wheel

The calculated results are shown as follows.

$$W_T = 4.73\,[m].\ 0.87\,[kg/m] + 3.314\,[kg] + 9.4\,[m].\ 1.63\,[kg/m] + 8.2\,[kg] + 3.2\,[m]\ .\ 1.63\,[kg/m] + 12.43\,[m]\ .\ 1.63\,[kg/m] + 13\,[kg] + 250\,[kg]$$

$$W_T = 319.414\,[kg]$$

$$F\ wheel = (\frac{319{,}414}{4}),\ = 79{,}85\,[kg]$$

So, the selected wheel is a PU type with a size of 3" for a load of 80 [kg]

3.6. The final design of head loss testing equipment

Based on the design of the head loss testing equipment, the analysis has determined the specific loading forces acting on the frame. For the first frame series, the loading force was calculated to be 3.314 kg. For the second frame set, the loading forces include 3.15 kg for the 1-inch PVC pipe, 2.5 kg for the 1-inch galvanized pipe, and 1.3 kg for the 1-inch aluminum pipe. Additionally, the system includes a 13 kg load from a 108-bit Shimizu pump and 250 kg of water in the sump. These calculated loads are critical for ensuring that the frame design can adequately support the equipment during operation, confirming that the selected materials and design parameters are sufficient to maintain structural integrity under these conditions.

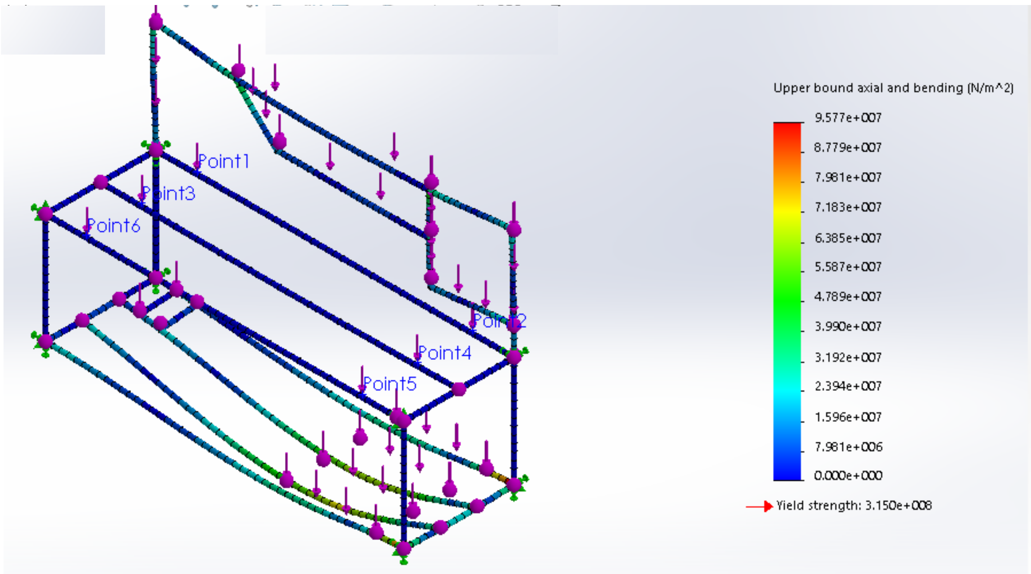

Figure 25. Load simulation for frame head loss testing equipment using SolidWorks Loading

Figure 26. Head loss testing equipment

4. Conclusions

The results of designing the frame for the flow loss test tool, it was found that the material used was ASTM A500 with a hollow size of 20 x 20 x 1.6 [mm] in the first frame, then a hollow of 35 x 35 x 1.6 [mm] in the frame second and third. From the loading design simulation results on the frame design of the Head loss testing equipment using SolidWorks, it is found that the safety factor value for dynamic loads is 2, it is safe to use in the design of the head loss test equipment frame.

The study successfully designed and validated a frame for head loss testing equipment, focusing on achieving a balance between strength, weight, and flexibility. The design process, which incorporated material strength analysis, detailed load calculations, and SolidWorks simulations, resulted in a frame capable of withstanding the operational loads with a safety factor of 2, ensuring its reliability and durability.

The use of ASTM A500 hollow sections was found to be optimal for this application, providing the necessary strength while keeping the frame lightweight. The simulations confirmed that the load distribution was well-managed, and the frame performed effectively under both static and dynamic conditions. The practical implementation of the design at Universitas Mercu Buana demonstrated its effectiveness, as the frame supported the head loss testing equipment without any significant issues, validating the design methodology.

In conclusion, this study provides a robust framework for designing frames for testing equipment in mechanical engineering applications. The combination of material strength analysis, careful specification selection, and advanced simulation tools proved to be an effective approach for ensuring the structural integrity and operational performance of the equipment. This methodology can be applied to similar engineering challenges, potentially improving the design and functionality of various mechanical systems. Future research could explore further optimization techniques or alternative materials to enhance the design further.

Acknowledgements

The author thanks to all those who have assisted in the preparation of this design article until finish. Especially, thank you very much also to Universitas Mercu Buana for financing to build the head loss Testing Equipment through funding for the Internal MBKM Research program even semester 2021/2022.

References

[1] Z. Zainudin, I. M. Adi Sayoga, and M. Nuarsa, “Analisa pengaruh variasi sudut sambungan belokan terhadap head losses aliran pipa,” *Din. Tek. Mesin*, vol. 2, no. 2, pp. 75–83, 2012, doi: 10.29303/d.v2i2.97.

[2] D. Krisdwiyanto and A. M. Akim, “Pengujian alat uji rugi-rugi aliran dalam pipagalvanis, pipa PVC, Pipastainless steel dan pipa acrylic,” *Zo. Mesin*, vol. 8, no. 2, pp. 35–45, 2017.

[3] Muchsin, “Kerugian-kerugian pada pipa lurus dengan variasi debit aliran,” *Jurnal Mekanikal,* vol. 4 no. 2, pp. 386-392, 2013.

[4] M. Adriana, A. A. B.P, and M. Masrianor, “Rancang bangun rangka (chasis) mobil listrik roda tiga kapasitas satu orang,” *J. Elem.*, vol. 4, no. 2, p. 129, 2017, doi: 10.34128/je.v4i2.64.

[5] A. Sadikin, “Perancangan rangka chasis mobil listrik untuk 4 penumpang menggunakan software 3D Siemens Nx8,” Thesis, Univ. Negeri Semarang, 2013.

[6] A. Pratama and M. Fitri, “Rancang bangun alat uji konstanta pegas untuk kapasitas 50 N/Mm menggunakan metode VDI 2221,” *AME (Aplikasi Mek. dan Energi) J. Ilm. Tek. Mesin*, vol. 6, no. 2, p. 41, 2020, doi: 10.32832/ame.v6i2.3316.

[7] A. Basri and M. Fitri, “Perancangan alat uji prestasi pompa menggunakan metode VDI 2221," *Jurnal Teknik Mesin,* vol. 10, no. 3, 2021.

[8] M. Fitri and F. Rizqiansyah, “Design of frame for the pump performance test equipment using VDI 2221 method,” *Int. J. Innov. Mech. Eng. Adv. Mater,* vol. 4, no. 1, pp. 17–22, 2022, doi: 10.22441/ijimeam.v4i1.15374

[9] Z. Pratama, “Desain komponen utama alat uji konstanta pegas untuk kapasitas 50 N/Mm,” *J. Tek. Mesin*, vol. 10, no. 1, p. 15, 2021, doi: 10.22441/jtm.v10i1.11108.

[10] M. Fitri, M. D. Heryanto, and D. M. Zago, “Aerodynamic analysis of fiberglass car body E-Falco.” *Jurnal Rekayasa Mesin,* vol. 12, no. 3, pp. 507–519, 2021, doi: 10.21776/ub.jrm.2021.012.03.2

[11] R.S. Khurmi and J.K. Gupta, *A Textbook of Machine Design*, S. Chand publishing, 2005.

[12] R. L. Mott, E. M. Vavrek, and J. Wang, *Machine Elements in Mechanical Design,* 6th Edition. Pearson Education, 2018.

[13] M. S. Ali, H. Praktikno, and W. L. Dhanistha, “Analisis pengaruh variasi sudut blasting dengan coating campuran epoxy dan aluminium serbuk terhadap kekuatan adhesi, prediksi laju korosi, dan morfologi pada plat baja ASTM A36,” *J. Tek. ITS*, vol. 8, no. 1, 2019, doi: 10.12962/j23373539.v8i1.39068.

[14] M. Min, Y. Liu, and K. Tousignant, "Design Thickness Requirements for Hollow Structural Sections." Thesis, Dalhoousie University, 2024.

[15] L. Edahwati, W.D. Lestari, S. Sutiyono, and T.P. Sari, *Modul Panduan Belajar Solidworks: 3D Model, Assembly, Drawing*, UPN Jatim, 2021. Available: https://repository.upnjatim.ac.id/7525/1/Modul_Solidwork_PKM_T.Mesin_UPN_Jatim.pdf.

[16] I. Sungkono, H. Irawan, and D.A. Patriawan, "Analisis desain rangka dan penggerak alat pembulat adonan kosmetik sistem putaran eksentrik menggunakan Solidwork," In *Prosiding Seminar Nasional Sains dan Teknologi Terapan*, vol. 1, no. 1, pp. 575-580, 2019.

[17] G.J. Hancock, T. Murray, and D.S. Ellifrit, *Cold-Formed Steel Structures to The AISI Specification*, CRC Press, 2021.